



DESIGN AND CHARACTERIZATION OF A FILM-FORMING GEL CONTAINING DOMPERIDONE-LOADED TRANSETHOSOMES FOR TRANSDERMAL DELIVERY

Samantha Neha Sequira and Sneh Priya*

Nitte (Deemed to be University), NGSIM Institute of Pharmaceutical Sciences (NGSIMIPS), Department of Pharmaceutics, Mangalore, India

This research aimed at formulating transethosomal film-forming gel (TG) of domperidone-an antiemetic and anti-sickness drug. The prepared transethosomes (TE) were optimized and the vesicle size, PDI and %EE of the optimized TE was 15.1nm, 0.387 and 73.82 respectively where the %error was $< \pm 5\%$ of the predicted value. The prepared formulation was further characterized for zeta potential, optical microscopy and transmission electron microscopy. The nano-vesicular systems were then incorporated into a film forming gel and evaluated for in vitro drug release and ex vivo skin permeation studies. The amount of drug released after 8 h for was found to be 49.67% for conventional gel (CG) and 36.079% for transethosomal gel (TG). TG followed first-order release kinetics and Higuchi model as the release mechanism. The steady-state flux of drug from TG after 8 h was found to be 2.51 times that of the CG. A skin irritation study was conducted using Wistar rats and the formulation showed no irritation to the skin. Stability testing was done and the formulation remained stable over the time period. It was concluded that domperidone-loaded TG can be a promising alternative for oral drug formulations due to the sustained release of the drug.

Keywords: Domperidone, film forming gel, transethosomes, nano-vesicular systems

INTRODUCTION

Cancer is a disease or a condition that develops when there is rapid and abnormal cell division. Cancer can be classified as benign-cancers that are localized in one part of the body and malignant- cancers that spread to other organs through blood flow¹. There are many clinically available drugs like chlorambucil, cyclophosphamide, 5-flourouracil, doxorubicin, epirubicin, docetaxel, paclitaxel etc that are used for adjuvant, neoadjuvant and metastatic cancer chemotherapy. These chemotherapeutic drugs are given by oral or by intravenous route as an injection or an infusion in the presence of a doctor or in a hospital². Anti cancer drugs are cytotoxic in nature and therapy with these drugs tends to show several side effects, the most common being nausea and vomiting, hair loss, change of taste, dry mouth, reduced appetite, constipation etc³.

Domperidone (DOM) is a dopamine-2

receptor antagonist drug that belongs to the class of prokinetics of antiemetic drugs. DOM increases the pressure of the lower oesophageal sphincter and also induces gastric emptying⁴. The antiemetic effect of DOM is due to its action on the motor activity of the stomach and small intestine, as well as on the chemoreceptor trigger zone⁵. The Biopharmaceutical Classification System (BCS) claims that DOM has been classified under class II category which is poorly soluble and highly permeable drugs⁶. DOM has very poor water solubility of about 1mg/ml and the oral bioavailability of DOM is 13-17%⁷. This very low oral bioavailability is mostly due to its hepatic first pass metabolism and also the gut wall metabolism. However, the bioavailability of DOM administered through intramuscular route is about 90%. The plasma half life of DOM is about 7.5 hrs and the adult dosage for oral route is 20 mg three to four times a day^{4,8}. DOM is known to have an efficient effect in prophylaxis of emesis and wide usage in

chemotherapy and radiotherapy but it can still cause problems to cancer patients when administered orally⁷.

Transdermal drug delivery system (TDDS) is a fast developing process that refers to the method of drug administration into the blood circulation by applying it to the skin. The drug passes through the stratum corneum, epidermis and the dermis layers of the skin without any accumulation. TDDS has many advantages like, bypasses hepatic first pass metabolism which is very common in case of oral drugs, pain free delivery of drugs, improves patient compliance, reduced dosing frequency, suitable for paediatric, geriatric, unconscious patients, etc.^{9,10}. The currently available different types of transdermal dosage forms like patches are occlusive in nature, prevent water loss from the skin surface, are difficult to apply to curved surfaces, cause pain while peeling off, cause discomfort and are also low aesthetics. Although semisolid preparations like ointment and creams help minimize these disadvantages they have certain limitations of their own like low skin contact time, need frequent application, greasy texture which in turn can cause poor patient compliance, easily washed or wiped off by the patient etc. Hence a novel approach at transdermal drug delivery called film forming gel which acts as a powerful substitute for traditional formulations has been developed. When applied to the skin or any other surface of the body, this is a non-solid sustained release dose form that forms a film. These systems contain a polymer that forms films, gelling agent and a volatile vehicle along with the drug and other excipients which after coming into touch with the skin, forms a clear film due to the evaporation of the solvent¹¹.

Liposomes are phospholipid drug carriers in the nano size range. These frequently build up in the stratum corneum layer and hence newer types of liposomes called deformable liposomes (DL) also called transferosomes have come into play. Transferosomes are liposomes that contain edge activators or permeation enhancers like span 60, tween 60 etc in order to reduce the drawbacks of conventional liposomes. Although the edge activators help DL to have higher permeability and flexibility when compared to CL, they cannot reach the deeper layers of the stratum corneum. Hence ethosomes came into existence by the addition of ethanol and water to liposomes in addition to their phospholipid envelop¹². Transethosomes (TE) is a novel

approach to liposomal formulation which has advantages of both ethosomes and transferosomes. These are lipid vesicular carriers of drugs that contain high amounts of ethanol and permeation enhancers or edge activators. They show irregular spherical shapes, high values of skin penetration and vesicular elasticity and hence they are also called ultra deformable vesicles (UDV)¹³.

Domperidone which is used to treat emesis has very low water solubility and poor oral bioavailability. It is generally administered through oral route which will be expelled out of the body due to further vomiting. The conventional oral route also involves hepatic first pass metabolism which can decrease the bioavailability of the drug. Furthermore, delivery of the drug through parenteral route or intramuscular route which has about 90% bioavailability can be painful and self-administration is not possible. Therefore there is a need of administering the drug by an alternative method like transdermal route. The transdermal drug delivery route not only helps in avoiding the drawbacks of conventional therapies but also helps in minimizing side effects and improving patient compliance. In this study, the incorporation of domperidone as phospholipid vesicles called transethosomes into a transdermal film forming gel with the purpose of sustained release of the drug and improving bioavailability of the drug is discussed.

MATERIALS AND METHODS

Chemicals and reagents

Domperidone and Chitosan were obtained from Yarrow Chem Products, Mumbai. Ethanol, Tween 20, Tween 80, Disodium hydrogen phosphate from LobaChemie, Mumbai, Propylene glycol and lactic acid were obtained from Merck, Mumbai. Unless otherwise, all chemicals and reagents employed were of analytical quality.

Formulation and characterization of TE

Design of experiments

To optimize the formulation, DOE was performed using Design Expert® software (version 11.0.3.0 64-bit, Stat-Ease, Inc. Minneapolis, MN, USA). The influence of the two independent variables, concentrations of soya lecithin and ethanol on Particle size, PDI, and %EE of TE was analysed using Central

Composite Design as shown in **Table 1**. The two levels included were low and high^{6,14,15}. The design presented 13 formulation runs as shown in **Table 2**.

Preparation of TE

Cold method was employed for the preparation of TE loaded with DOM^{16,17}. 2% w/v of soya lecithin, 100mg of drug, 35% v/v of ethanol and 0.2% w/v of tween 20 was stirred on a magnetic stirrer by maintaining 30°C on a water bath. An aqueous phase composed of double distilled water at 30°C was injected into the organic phase in a fine stream. Stirring was continued for 45 min. The product was further sonicated for 30 min using ultrasonic probe sonicator.

Vesicle size, size distribution and zeta potential

Zeta sizer (Nano ZS, Malvern Instruments, UK) was used to measure TE's particle size and size distribution by dynamic light scattering. 1ml of transethosomal suspension (TS) was

diluted in 10ml of double distilled water. This suspension with dilution factor of 0.1 was measured for particle size using the zeta sizer. A particle's ZP is the total charge that particles acquire in a specific medium. The stability of the formulation can also be determined with the help of ZP value¹⁶.

Percentage drug entrapment efficiency (%EE)

10 ml of TS was taken in a 15 ml Tarsus centrifuge tube and centrifuged at 13,000 rpm and 4°C for 60 min by cold centrifugation. The supernatant was separated from the sediment during centrifugation and was analysed for DOM concentrations at 284 nm using the UV spectroscopic method. The %EE was calculated using the equation 1¹⁷.

% Entrapment efficiency =

$$\frac{\text{Total amount of drug added} - \text{unentrapped drug}}{\text{Total drug added}} \times 100 \quad (1)$$

Table 1: Factors and levels.

Independent factors	Levels		Dependent factors	Goal
	Low	High		
Soya lecithin (X ₁)(% w/v)	2	4	Vesicle size (Y ₁)(nm)	100-120
Ethanol (X ₂)(% v/v)	25	35	PDI (Y ₂)	<0.3
			Entrapment Efficiency (Y ₃)(%)	>75

Table 2: Composition of transethosomes as given by Central Composite Design using Design of Experiment software.

Std Code	Drug (mg)	Soya lecithin %w/v	Ethanol concentration %v/v	Tween 20 concentration %w/v
1	100	2	25	0.2
2	100	4	25	0.2
3	100	2	35	0.2
4	100	4	35	0.2
5	100	1.59	30	0.2
6	100	4.41	30	0.2
7	100	3	22.9	0.2
8	100	3	37.07	0.2
9	100	3	30	0.2
10	100	3	30	0.2
11	100	3	30	0.2
12	100	3	30	0.2
13	100	3	30	0.2

Formulation and characterization of optimized batch of TE

One-way ANOVA was applied using the commercially accessible software program Design-Expert version 11 to evaluate the effect of process variables on the responses and to refine the parameters for the formulation. The optimization of TE was carried out using constraints with minimum particle size, minimum PDI and maximum %EE and the solution with very good desirability (greater than 0.9) was suggested by the software which was selected as optimized formulation. 2% w/v soya lecithin and 33.697% v/v of ethanol is used to formulate the optimized formulation. Vesicle size, size distribution and ZP, and %EE of optimized formulation are achieved in the same way as other batches. Shape and surface morphology was determined by Optical High-Resolution Microscopy and Transmission Electron Microscopy.

Shape and morphology analysis

High-power Optical microscope (BIOVIS particle analyzer) and Transmission Electron Microscopy (TEM) was used to determine the shape and surface morphology of the TE^{18,19,20}.

Elasticity test

Extrusion technique was used for the measurement of elasticity of optimized TE by using a polycarbonate membrane having pore diameter of 200nm, 25mm diameter filters of 200ml capacity barrel which was driven by an external pressure of 2.5 bars²¹. The equation 2 was used to calculate deformability index:

$$D = \frac{J}{t} \times \left(\frac{r_y}{r_p}\right)^2 \quad (2)$$

where, D = Deformability index (ml/s), J = amount of suspension extruded (ml), t = extrusion time (s), r_y = vesicle size after extrusion (nm), r_p = pore size of the extrusion membrane (nm)

Preparation of DOM loaded transethosomal film-forming gel (TG)

1% TG was prepared by incorporating a required quantity of the DOM loaded TE into a gel base. Chitosan was dispersed in distilled water for 15 minutes to create the gel base. Subsequently, lactic acid, propylene glycol, tween 80 and ethanol were added. Similarly a conventional film forming gel (CG) was

prepared by incorporating an alcoholic solution of pure drug (PS) to the gel base.

Characterization of DOM loaded TG

Determination of pH

1g gel was weighed and dilute with distilled water to 100 ml. The pH of both gels is calculated by submerging the electronic pH metre for 1 minute to bring it into equilibrium with the solution²².

Viscosity

Brookfield Viscometer DV-II+pro, D220 with spindle number T-96 and 10, 20, 50 and 100rpm speed was employed to measure the viscosity of both the gels²³.

Spreadability

The spreadability of both TG and CG was measured using modified wooden block and glass slide equipment. 1g gel was measured on the ground slide and was sandwiched using another slide which was then fitted with the hook. To remove air and create a clear gel coating between the slides, a 100g weight was placed on them for five minutes. The excess gel was scraped out from the corners. Using the string connected to the handle, 30g of pull was applied in order to move the top plate to 5 cm distance and the time (sec) taken is noted. The equation 3 was used to measure spreadability:

$$S = \frac{M \times L}{T} \quad (3)$$

Where S = is the spreadability, M = is the weight in the pan (attached to the upper slide), L = is the length transferred by the glass slide and T = reflects the time required to remove the slide entirely from each other²⁴.

Drug content

1g of the TG was dissolved in a 100 ml volumetric flask containing 10 ml of pH 6.8 phosphate buffer. The solution was made upto 100ml with phosphate buffer pH 6.8 to give a solution with concentration of 100µg/ml. 0.5ml was pipette out from this solution into a 10ml volumetric flask and volume was made up using pH 6.8 phosphate buffer. After filtration, the drug was estimated spectrophotometrically at wavelength of 284 nm and the drug content was determined²⁵.

Drug- excipient compatibility study by FTIR

The IR spectrum of the final optimised formulation of TG was compared to the IR spectrum of DOM in order to examine how the chemical makeup of the drug changes when it is combined with excipients. The characteristic peak wave numbers of the formulation were compared with the pure sample and interpreted²⁶.

***In vitro* drug release study of different formulations**

A comparative *in vitro* drug release study for PS and TS was carried out using dialysis technique^{27,28}. Prior to this, phosphate buffer pH 6.8 was used to soak the dialysis membrane for 24 hrs. Skin pH is slightly acidic and ranges from anywhere between 4-7; hence pH 6.8 buffer is used to mimic skin pH²⁹. The PS and optimized TS equivalent to 5mg of drug were taken in two dialysis membranes, respectively. Each membrane was tied from both ends like a bag which was then tied to a glass rod and suspended vertically. It was then submerged in a beaker containing 100ml of pH 6.8 buffer and a tiny magnetic bead rotating at a speed of 50 rpm. The study was carried out at 37± 0.5°C for 8 hrs. At predetermined time intervals, 1ml of sample was withdrawn from reservoir compartment which was suitably diluted and analysed spectrophotometrically at 284 nm. In order to maintain sink condition, the amount of sample withdrawn was replaced with the same quantity of phosphate buffer of pH 6.8. The *in vitro* drug release study for CG and TG was carried out similarly. An amount of CG containing pure drug and TG loaded with DOM equivalent to 5mg of drug was added to each dialysis membrane respectively.

***In vitro* drug release kinetics**

Kinetic analysis was performed for the first order (log cumulative percentage drug vs time) and zero order kinetics (cumulative amount of drug unreleased vs time) using the data obtained from the drug release study. Mechanism of drug released was determined by fitting the data to Korsmeyer-Peppas (log cumulative percentage drug released vs log time) and Higuchi's matrix model (cumulative percentage drug released vs square root of time)²⁸.

***Ex vivo* skin permeation study of different formulation**

Porcine skin is the greatest substitute for human skin since it is highly vascularized and relatively thin. Additionally, its lipid content is close to that of human skin^{30,31}. The fresh porcine skin was procured from local slaughter house and cleaned well so as to obtain a hairless skin and kept in phosphate buffer pH 6.8. The *ex vivo* skin experiments were performed using two compartments containing Franz Diffusion cell²⁸. The donor compartment consists of two open ends where one end is covered with porcine skin previously soaked in phosphate buffer pH 6.8 with the dermal side facing up towards the donor compartment. PS and TS equivalent to 5mg of drug were added to each of the donor compartments respectively. Reservoir compartment was loaded with 12 ml pH 6.8 phosphate buffer containing a small rotating magnetic bead at a steady 50 rpm speed. The study was performed for 8 hrs at 37± 0.5°C. At a fixed time period, 5ml of samples were collected from the reservoir compartment which was suitably diluted and the absorbance was determined spectrophotometrically at 284nm. In order to maintain sink condition, the amount of sample withdrawn was replaced with the same quantity of phosphate buffer of pH 6.8. The *ex vivo* skin permeation study for CG and TG was carried out similarly. An amount of CG and TG loaded with DOM equivalent to 5mg of drug was applied to dermal side of each skin respectively.

Calculation of skin permeation parameters

Cumulative amount of drug permeated per unit area was calculated as a function of time. The linear portion of the slope gave the flux. The DOM permeability coefficient (K_p) through porcine skin was calculated using the relationship established by the first law of Fick's diffusion, which is represented by equation 4:

$$K_p = \frac{J}{C} \quad (4)$$

Where J is the flux and C is the drug concentration in donor compartment³².

Skin deposition study

In order to remove excess DOM from the skin surface, the skin surface was cleansed five times with 5ml of methanol after the 24 h skin permeation study was complete. The skin was then cut into small fragments and added to 5ml

of methanol followed by sonication for 10mins. The solution was centrifuged for 15mins at 10,000 rpm. DOM content in the supernatant was analysed using UV-visible spectrophotometer at 284 nm³³.

***In vivo* skin irritation study**

A study was carried out to know whether the film can cause any irritation and Wistar rat skin was preferred for this purpose since it is very permeable. Its skin structure resembles to that of human skin and the animals can be easily procured. The animals were anaesthetized and 24hrs before application of the sample, the back of the animals was shaved using a razor to remove all the fur. It was done carefully to prevent any skin damage that would change the permeability of the skin.. The shaved area was subsequently treated with methylated spirit as an antiseptic using cotton wool to avoid infections and TG was topically applied for each group of rats. The test material was removed after 24hrs and the surface of the skin was rinsed with distilled water. Observation of the site was done at 24hrs and 48 h after application of the formulation^{34,35}.

Stability studies

The prepared TG were stored at 25± 2°C having a relative humidity of 60% storage condition to analyze its stability according to ICH guidelines³⁶. Sampling was done and the gel was assessed for appearance, drug content and drug release at the end of four weeks.

Statistical analysis of data

Multiple statistical assessments were done using unpaired t-test using Graph Pad Prism software. All the data are considered as mean with standard deviation values (mean±SD) with n=3. The significance was considered at p< 0.05.

RESULTS AND DISCUSSIONS

Results

Statistical analysis

The TE loaded with DOM were developed using the method described in the procedure. Central Composite Design to understand the effects of the transethosomal constituents i.e. the soya lecithin and ethanol on its attributes,

particle size, PDI and %EE and response is shown in **Table 3**.

Particle size of TE

Vesicle size significantly influences how well TE permeates skin. The independent variables i.e., concentration of soya lecithin and concentration of ethanol showed significant effects on vesicle size as depicted in the perturbation plot and 3D graph (**Fig. 1 and Fig. 2**). The Central Composite Design showed that increase in soya lecithin concentration from 2 to 4% w/v, there was an increase in vesicle size at all concentrations of ethanol. This may be due to enhanced viscosity of the TS and thickness of lipid bilayers³⁶. As the concentration of ethanol increased from 25 to 35% v/v initially there was an increase in vesicle size up to certain concentration and then the vesicle size decreased at all concentrations of soya lecithin. Reduced membrane thickness and the development of a phase with interpenetrating hydrocarbon chains both contribute to a reduction in TE's size³⁷. As shown in **Table 4**, The model created for vesicle size had a p value of <0.0001 and a F value of 52.30, which showed that the quadratic model was significant. The vesicle size may be determined using the model as the F-value of 3.77 indicates a non-significant lack of fit. The discrepancy between the Predicted R2 of 0.8524 and the Adjusted R2 of 0.9553 is less than 0.2. The polynomial equation obtained is:

$$\text{Vesicle Size} = +143.05 + 12.17(A)^* + 9.51(B)^* - 8.72(AB)^* - 5.98(A^2) - 38.31(B^2)^*$$

Where A and B are the concentrations of soya lecithin and ethanol respectively. The coefficient in this equation reflects the standardized beta coefficient and the asterisk symbol implies variable significance. The synergistic impact is represented by a positive sign, whereas the antagonistic effect is represented by a negative sign. Inferred from the polynomial equation, an A coefficient that is positive, represents the increase in vesicle size with an increase in concentration of soya lecithin, while B coefficient that is also positive shows an increase in vesicle size with the increase in ethanol concentration.

Table 3: Result of response of transethosomes as per Central Composite Design using Design of Experiment Software.

Form. Code	*Vesicle Size \pm SD (nm) Y ₁	*PDI \pm SD Y ₂	*Entrapment Efficiency \pm SD(%) Y ₃
1	63.58 \pm 3.01	0.323 \pm 0.08	68.8 \pm 2.04
2	102.95 \pm 2.42	0.54 \pm 0.065	75.36 \pm 2.64
3	110.8 \pm 2.34	0.271 \pm 0.06	72.9 \pm 2.49
4	115.3 \pm 4.09	0.483 \pm 0.041	70.1 \pm 3.69
5	112.8 \pm 3.55	0.253 \pm 0.079	79.52 \pm 3.15
6	150.6 \pm 2.48	0.572 \pm 0.079	82.7 \pm 2.23
7	61.2 \pm 3.07	0.47 \pm 0.028	64.81 \pm 2.64
8	72.9 \pm 4.45	0.502 \pm 0.057	60.94 \pm 3.09
9	142.51 \pm 3.54	0.391 \pm 0.048	75.1 \pm 4.69
10	148.2 \pm 2.23	0.428 \pm 0.024	77.9 \pm 3.47
11	137.22 \pm 3.06	0.62 \pm 0.057	76.21 \pm 4.06
12	147.22 \pm 2.51	0.54 \pm 0.016	75.4 \pm 4.38
13	140.11 \pm 2.01	0.59 \pm 0.22	75.98 \pm 2.27

*Average of three determinants; SD = Standard Deviation.

Table 4: Summary of regression analysis and ANOVA.

Sl. No	Factor	Vesicle size (Adjusted R ² = 0.9553)		PDI (Adjusted R ² = 0.4738)		% EE (Adjusted R ² = 0.9712)	
		Estimated beta coefficient	P value	Estimated beta coefficient	P value	Estimated beta coefficient	P value
1.	Intercept	143.05	<0.0001*	0.4602	0.0162*	76.12	<0.0001*
2.	A-Soya lecithin	12.17	0.0016*	0.1100	0.0051*	1.03	0.0239*
3.	B-Ethanol	9.51	0.0059*	-0.0080	0.8013	-0.8291	0.0544
4.	AB	-8.72	0.0393*	-	-	-2.34	0.0025*
5.	A ²	-5.98	0.0560	-	-	2.45	0.0004*
6.	B ²	38.31	<0.0001*	-	-	-6.67	<0.0001*

*Represents p-values <0.05 which are significant toward the response.

PDI of TE

The width of unimodal size distributions is measured by PDI. An completely heterogeneous polydisperse population is indicated by a value of 1, while homogeneous dispersion is indicated by a value of 0. A PDI value of less than 0.5 is considered acceptable³⁸. Concentration of soya lecithin and concentration of ethanol showed significant effects on PDI as depicted in the perturbation plot and 3D graph (**Fig. 1 and Fig. 2**). With a p-value of 0.0162 and F value of 6.40, the linear model generated for PDI was significant. According to the F-value of 0.5937, the lack of fit is not statistically significant, indicating that the model can be used to calculate the PDI. As shown in Table 4, the discrepancy between the Predicted R² value of 0.3574 and the Adjusted R² value of 0.4738 is less than 0.2. The polynomial equation obtained:

$$PDI = + 0.4602 + 0.1100(A)^* - 0.0080(B)$$
 Where A and B are the concentrations of soya

lecithin and ethanol respectively. The coefficient in this equation reflects the standardized beta coefficient and the asterisk symbol implies variable significance. The polynomial equation shows that there is positive effect of soya lecithin concentration on PDI.

%EE of TE

The perturbation graph and 3D Response surface graph (**Fig. 1 and Fig. 2**) demonstrates that a rise in soya lecithin concentration as well as %EE of the drug. This effect may be attributed to enhancement of in lipid viscosity with increasing phospholipid concentration. There is an increase in hydrophobicity and alkyl chain lengths which help in preventing the drug from leaching out¹⁴. Initially, the %EE increases with an increasing ethanol concentration followed by a decline. Ethanol increases the fluidity of the membrane which is the reason for the initial rise in the %EE. The gradual fall in the

%EE was due to increase in ethanol concentration which made the vesicle membrane leaky³⁹. According to **Table 4**, the model created for %EE had a p value of < 0.0001 and an F value of 81.99, showing that the quadratic model was significant. The F-value of 0.6021 shows that the lack of fit is not statistically significant, indicating that the model can be used to calculate the %EE. The discrepancy between the Predicted R² of 0.9419 and the Adjusted R² of 0.9712 is less than 0.2. The polynomial equation obtained:

$$EE = + 76.12 + 1.03 (A)^* - 0.8291 (B) - 2.34 (AB)^* + 2.45 (A2)^* - 6.67 (B2)^*$$

Where A is the concentration of soya lecithin, B is the concentration of ethanol, the coefficient in this equation reflects the standardized beta coefficient and the asterisk symbol implies variable significance. The polynomial equation shows that there is positive effect of soya lecithin concentration on the %EE.

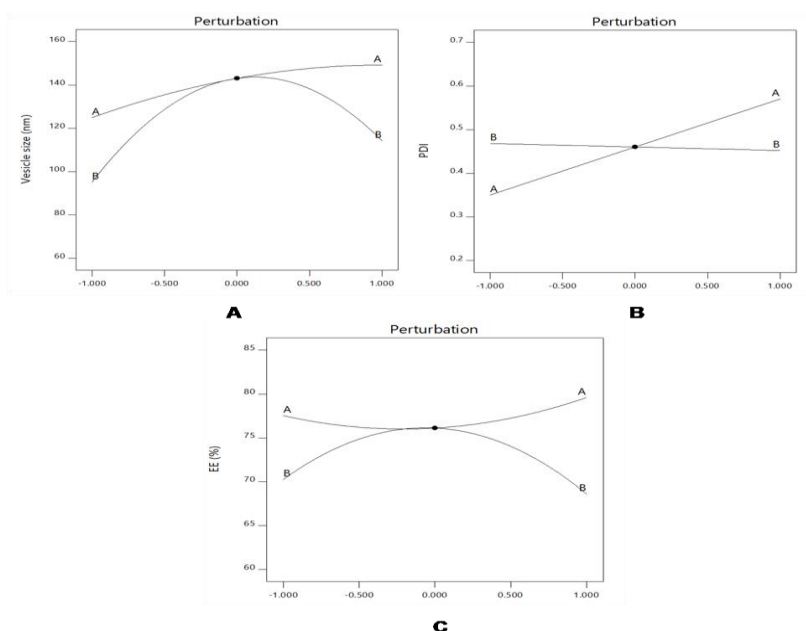


Fig. 1: Perturbation plot representing effect of soya lecithin and ethanol on A) vesicle size B) PDI C) entrapment efficiency.

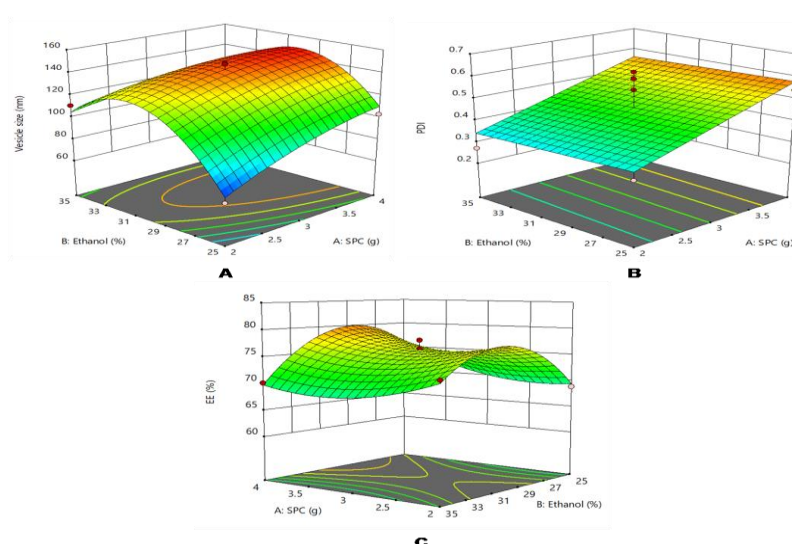


Fig. 2: 3D response surface curve representing effect of soya lecithin and ethanol on A) vesicle size B) PDI C) entrapment efficiency.

Optimization of TE

The optimization done according to every response; taking into consideration minimum particle size, PDI and maximum %EE. The solution given by the software containing 2% w/v soya lecithin and 33.697% v/v ethanol was utilized to prepared the optimized formula (F_{opt}). The observed value of vesicle size, PDI and %EE was found to be 115.1nm, 0.321 and 75% as shown in **Fig. 3** with percentage error $< \pm 5\%$ of the predicted value which is acceptable.

ZP of TE

The ZP of the F_{opt} was found to be -16.55 mV as shown in **Fig. 4**. The ZP of TE showed a negative value, due to the presence of ethanol. Ethanol also provides certain degree of physical stability to the vesicles, thus preventing aggregation. A crucial factor that can affect both vesicular characteristics like stability and skin-vesicle interactions is the charge of TE.³⁷.

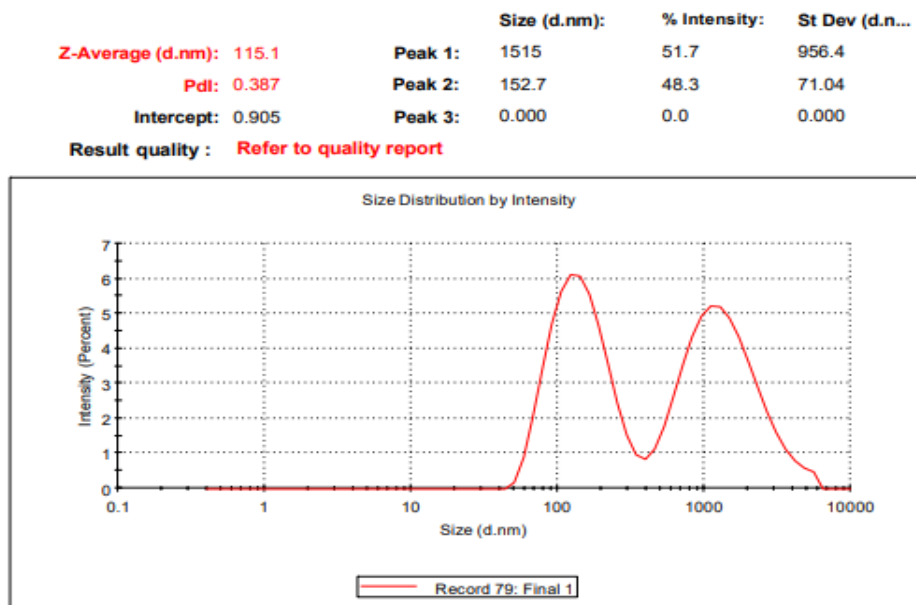


Fig. 3: Size distribution of optimized formulation of transethosomes (F_{opt}).

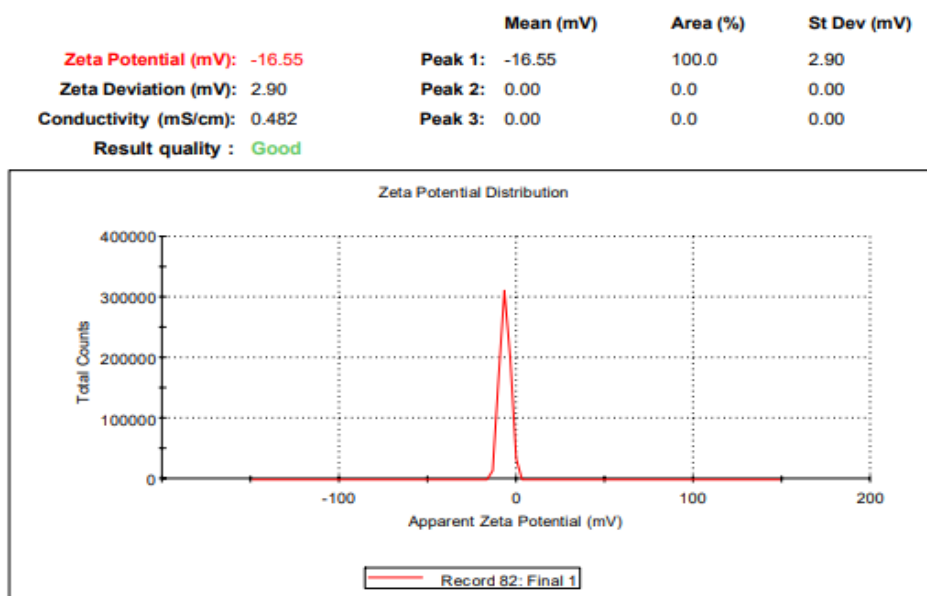


Fig. 4: Zeta potential of optimized formulation of transethosomes (F_{opt}).

Shape and Morphology of TE

From optical photomicrography (**Fig. 5**), it was clear that large number of bilayered TE were formed which were uniform in size and spherical in shape. The TEM images provided in **Fig. 6** displayed the surface morphology of vesicles with the presence of a unilamellar vesicular structure.

Elasticity test

TE were found to have a deformability index 13.23ml/s with standard deviation of 0.242. TE are highly elastic in nature and the presence of ethanol as well as tween 20, an edge activator imparts higher deformability to TE^{13,40}.

Preparation of DOM loaded TG

1% TG and CG was formulated which contained 3% w/w shrimp shell chitosan and 2% w/w propylene glycol. These act as viscosity inducing agents and gelling agents. The gel base was formed by adding 4% w/w lactic acid to chitosan and propylene glycol mixture followed by 5% w/v of tween 80 which acts as a skin permeation enhancer. DOM loaded TG was prepared by adding the prepared transethosomes to the gel base, and this prepared TG was opaque and free of any foreign substance⁴¹.

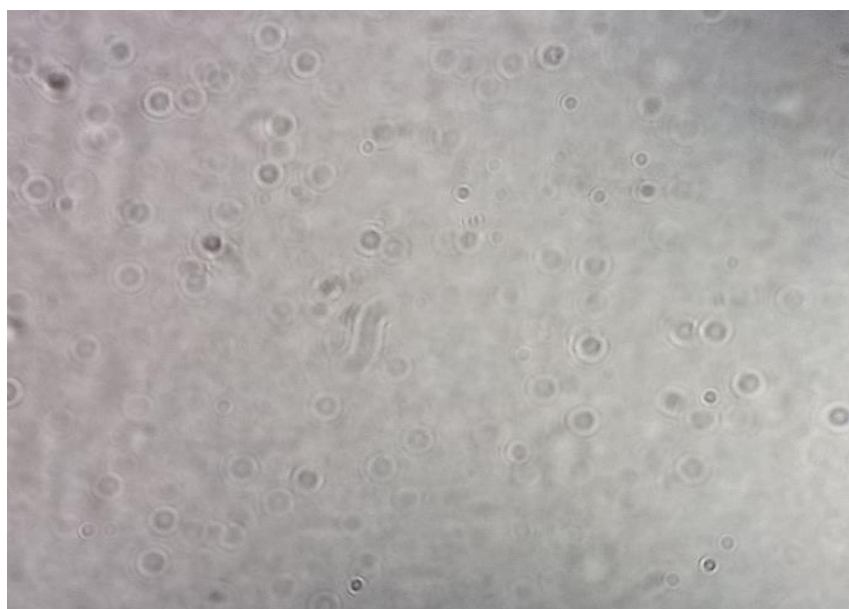


Fig. 5: Microscopic image of vesicles under high power microscope (F_{opt}).

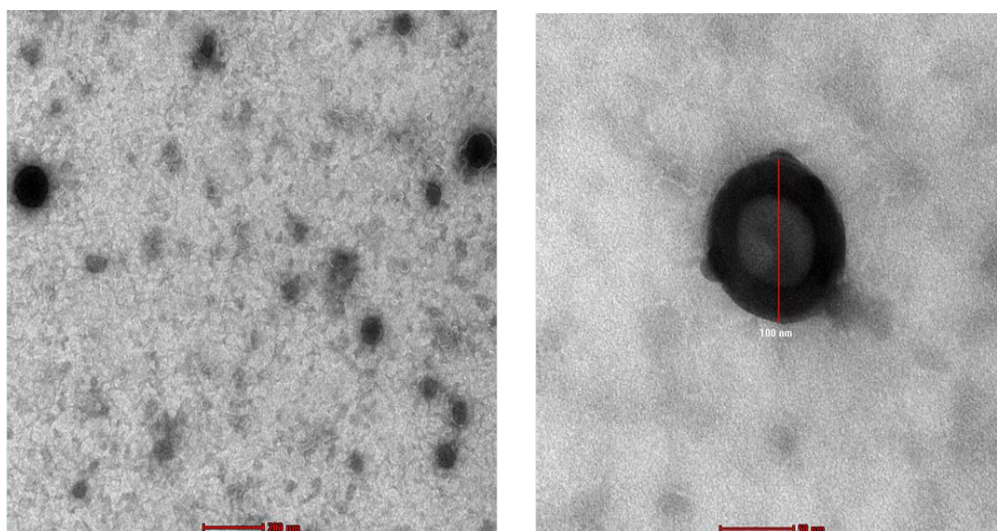


Fig.6: TEM images of optimized transethosomal vesicle (F_{opt}).

Characterization of DOM loaded TG

As mentioned in **Table 5**, the optimized TG was found to be yellowish, off-white, smooth and uniform in appearance. The spreadability of the TG was found to be 15.61 g/cm² showing that the gel has good spreadability and can spread easily with a small amount of shear. The pH of the TG was found to be 6.8. The formulation's pH should be as similar to the skin's pH in order to avoid skin irritation. The pH of the optimized TG was found to be within the range of skin pH; hence, no skin irritation was expected. The drug content of the TG was found to be 97±1.273%. The standard deviation (1.273) was found to be very less ensuring good uniformity of drug in the TG.

Viscosity

Brookfield viscometer was used to determine the viscosity of the CG and TG at 10, 20, 50, 100 rpm. The viscosity of the formulation ranged between 441-52 cps for CG and 538-79 cps for TG as shown in **Table 6**. The higher viscosity of TG may be attributed to the phospholipid content which is absent in CG¹⁶. As shown in **Fig. 7** and based on the data collected a rheogram was developed. It revealed that the formulations exhibited shear thinning effects. Pseudoplastic behavior has been observed i.e. increase in shear rate causes increase in viscosity.

Table 5: Data on appearance, spreadability, pH and drug content of the transethosomal film forming gel.

Form. Code	Properties			
	Appearance	*pH	*Spreadability (gm/cm ²)	*Drug content (%)
CG	Yellowish, off-white color, smooth	6.8 ± 0.24	17.904 ± 1.68	96 ± 1.89
TG	Yellowish in color, smooth	6.8 ± 0.17	15.61 ± 1.324	97 ± 1.273

*Average of three determinants; SD = Standard Deviation, CG: Conventional gel, TG: Transethosomal gel.

Table 6: Results obtained from viscosity studies.

Form. code	*Viscosity ± SD (cps)			
	10 RPM	20 RPM	50 RPM	100 RPM
CG	441 ± 3.51	272 ± 2.34	105 ± 3.65	52 ± 3.42
TG	538 ± 2.36	325 ± 2.48	157 ± 3.15	79 ± 3.01

*Average of three determinants; SD = Standard Deviation CG: Conventional gel, TG: Transethosomal gel.

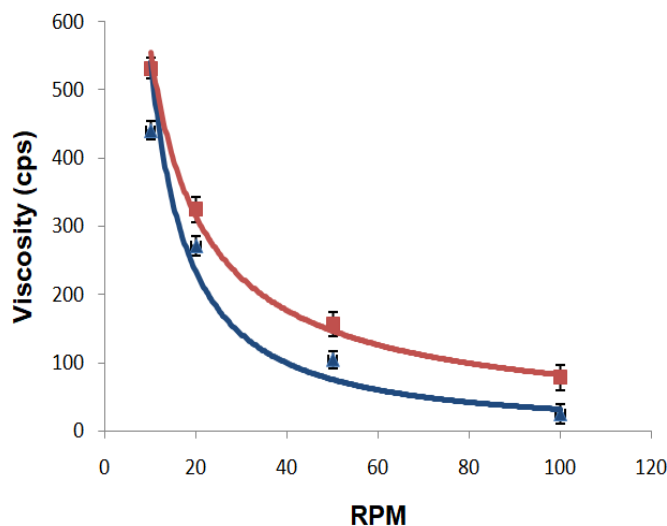


Fig. 7: Rheogram of transethosomal and conventional gels.

Drug-excipient compatibility study by FTIR

To determine whether the drug and the excipients were compatible, an FTIR study was performed. The pure drug's spectrum and the TG are shown in Fig. 8 and major peak values are

shown in Table 7. The principle peaks of drug were present in final formulations, this demonstrates that the drug and the employed excipients are compatible.

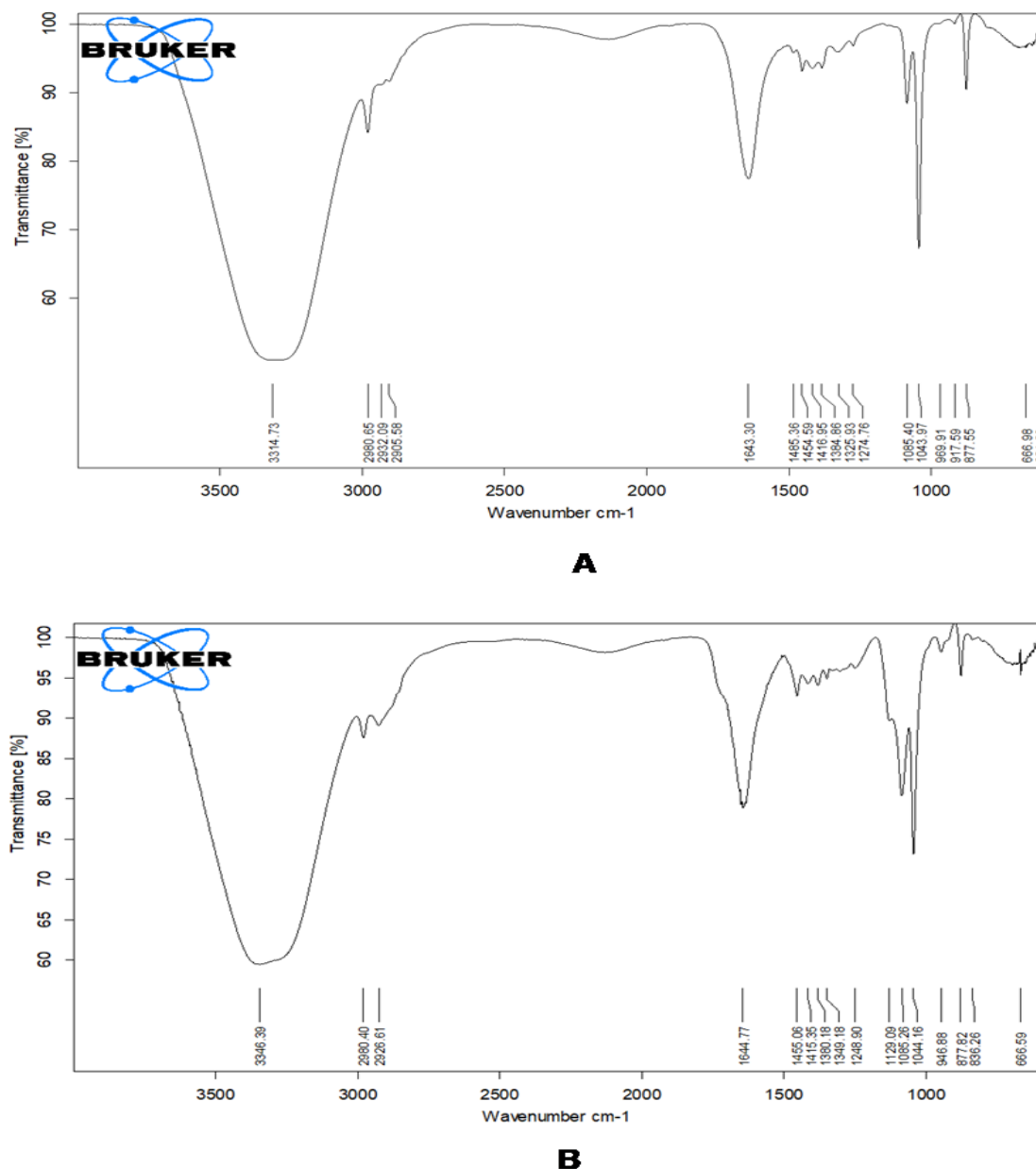


Fig. 8: FTIR spectrum of A) optimized transethosomal suspension of domperidone B) transethosomal film forming gel of domperidone.

Table 7: Major IR peaks of pure domperidone and transethosomal film forming gel.

Composition	Major Peak (wave numbers cm^{-1})
Pure domperidone	3025.06, 2818.07, 1715.31, 1694.22, 1489.15, 1147.18, 1062.18.
Transethosomal film forming gel	3240.39, 2926.61, 1644.77, 1455.06, 1129.09, 1085.26, 1044.16.

In vitro drug release study of different formulations

In vitro drug release profile of different formulations is shown in **Fig. 9**. By this, we can infer that in comparison to the PS, the release of DOM over the dialysis membrane was noticeably prolonged by its encapsulation into TE. The drug released from the TS after 8 h was 76.396% when compared to the PS which showed a release of 96.109%. After 8 hrs, it was discovered that the highest amount of drug released from the CG was 49.67% whereas in case of TG the drug release was 36.079%. The release was slower and sustained as the drug first diffuses from the transethosomal carrier followed by diffusion from the gel⁴².

In vitro drug release kinetics

The release kinetics of the different formulations was analyzed by using various kinetic models. The data analysis was focused on the corresponding significance of the regression coefficients. The result in **Table 8** shows that all formulations followed first order kinetics. The drug release mechanism of all the formulations was studied by fitting the data to Higuchi model and Korsmeyer-Peppas exponential model. The drug release mechanism of the PS as well as the optimized TS followed Korsmeyer-Peppas model as the regression coefficient (R^2) was higher than Higuchi model. The release exponent (n) of the formulations was found to be above 0.45 which indicates that the release can be defined by Non-Fickian diffusion, which may mean that more than one process regulates the release rates of drugs, i.e. diffusion coupled with erosion mechanism. As the value

of regression coefficient (R^2) of Higuchi model was found to be higher than that of Korsmeyer-Peppas model, both the CG and TG followed Higuchi model as drug release mechanism which in turn shows that the drug is released by matrix diffusion. The gel swells upon contact with fluid which causes the drug to diffuse through the matrix^{43,44}.

Ex vivo skin permeation study of different formulations

The amount of drug permeated through the porcine skin was evaluated using ex vivo study. The obtained release profile shows that there is enhanced permeation of TE as compared to the pure drug. Phospholipid vesicles, ethanol, and skin lipids all work together in a synergy. The stratum corneum lipids are fluidized by ethanol which enhances drug permeation. Ethanol also increases the lipid fluidity of lipid carriers and makes them flexible. The medication is released as a result of the fusion of TE with skin lipids as these flexible vesicles force their way past the stratum corneum into the deeper layers of skin^{13,33}. At the end of 8 h, higher percent cumulative permeation of 58.47% for TS was observed than PS which was 24.67%. In case of TG, higher permeation of 48.20% was seen than the CG which was 19.7% as DOM was encapsulated within the TE which imparted a lipophilic nature which is a prerequisite for a molecule to cross the biological membrane. In addition, the permeation profile of TG indicated a slow release as compared to TS as in case of TG, the drug has to first diffuse from the nano-vesicle in which it is entrapped in followed by diffusion through the gel matrix⁴⁵.

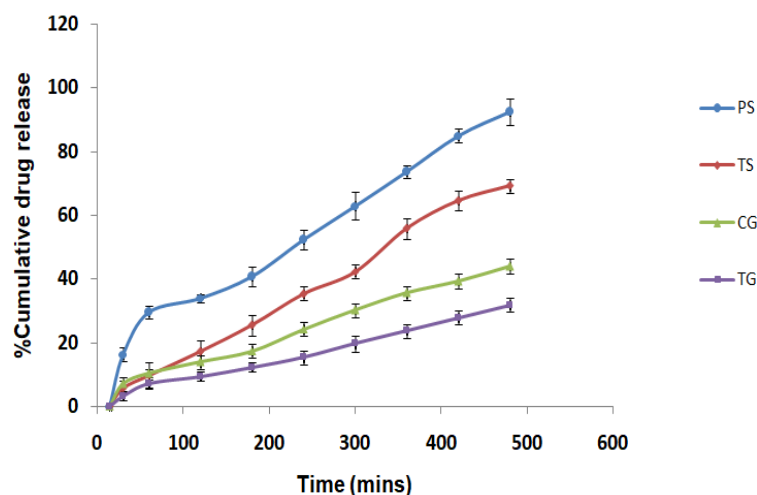


Fig. 9: Comparative *in vitro* drug release study of different formulations.

Calculation of skin permeability parameter

As shown in **Table 8** and **Fig. 10**, the cumulative amount of drug permeated through porcine skin after 8 h for PS (757.158 $\mu\text{g}/\text{cm}^2$) was lower compared to vesicular systems, particularly TS (1651.78 $\mu\text{g}/\text{cm}^2$). The cumulative amount of drug permeated through porcine skin after 8 hrs for CG (559 $\mu\text{g}/\text{cm}^2$) was lower compared to TG (1361.86 $\mu\text{g}/\text{cm}^2$). The results were found to be significant ($p < 0.05$). Both these results suggest that vesicular systems could improve the transdermal delivery of DOM. TS had a larger steady state flux than PS, and the same was observed for TG and CG. It was discovered that steady state flux and permeability coefficients have a direct relationship. Higher flux was observed for TE in comparison pure drug because ethanol, phospholipid vesicles, edge activator, and skin lipids interacted synergistically to increase the drug's transit through pig skin³³. The outcomes could also be attributed to the TE's remarkable deformability and flexibility, which enabled them to get beyond the skin barrier qualities⁴⁰.

Skin deposition study

As shown in **Table 9**, higher skin deposition of TS (225.19 $\mu\text{g}/\text{cm}^2$) than PS (130.67 $\mu\text{g}/\text{cm}^2$) and TG (294.49 $\mu\text{g}/\text{cm}^2$) than CG (159.43 $\mu\text{g}/\text{cm}^2$) was obtained as the result of combined effect of phospholipid, ethanol and edge activator skin, thus acting as a depot and helping in sustained delivery of drug for extended period of time⁴⁶.

In vivo skin irritation study

The TG was tested for skin irritation using Wistar rats, and as results shown in **Fig. 11**, it was observed that no rats showed signs of skin irritation or erythema. Thus the TG was safe for application on the skin.

Stability Studies

For 4 weeks, TG stability experiments were conducted in accordance with ICH guidelines. According to the results obtained in **Table 10**, no significant changes in the parameters were found when compared to the original formulation.

Table 8: Comparison of in vitro drug release kinetics.

Form. code	Kinetic models								
	Zero order		First order		Higuchi		Korsmeyer-Peppas		
	R ²	K	R ²	K	R ²	K	R ²	K	n
PS	0.933	0.181	0.952	-0.002	0.948	4.341	0.985	0.222	0.681
TS	0.986	0.157	0.988	-0.0001	0.969	3.657	0.997	-0.037	0.710
CG	0.979	0.094	0.991	-0.0003	0.991	2.313	0.979	0.54	0.604
TG	0.985	0.069	0.989	-0.0005	0.982	1.602	0.963	-0.067	0.581

PS: Pure drug solution, TS: Transethosomal suspension, CG: Conventional gel, TG: Transethosomal gel.

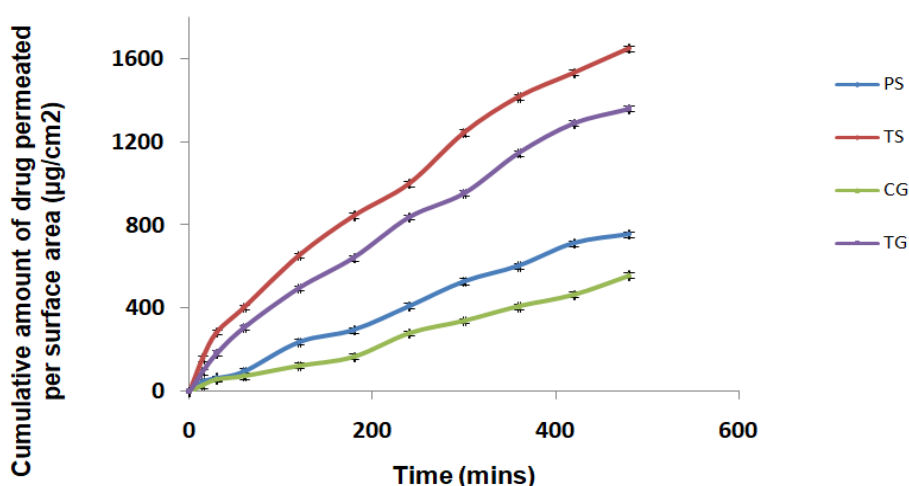


Fig. 10: Ex vivo skin permeation from the different formulations through porcine skin.

Table 9: Permeated amount of domperidone at 480 mins, flux, permeability coefficient and skin retention value.

Form. Code	*Permeated amount \pm SD at 480 mins ($\mu\text{g}/\text{cm}^2$)	Flux ($\mu\text{g}/\text{cm}^2 \cdot \text{min}$)	Permeability constant (K_p) $\times 10^{-3}$ (cm/h)	Amount of drug deposited in the skin ($\mu\text{g}/\text{cm}^2$)
PS	737.158 \pm 15.5	1.616	0.3232	130.67
TS	1651.78 \pm 16.75	3.350	0.67	225.19
CG	519.90 \pm 13.46	1.122	0.2244	159.43
TG	1361.86 \pm 16.81	2.825	0.565	294.49

*Average of three determinants; SD = Standard Deviation PS: Pure drug solution, TS: Transethosomal suspension, CG: Conventional gel, TG: Transethosomal gel.

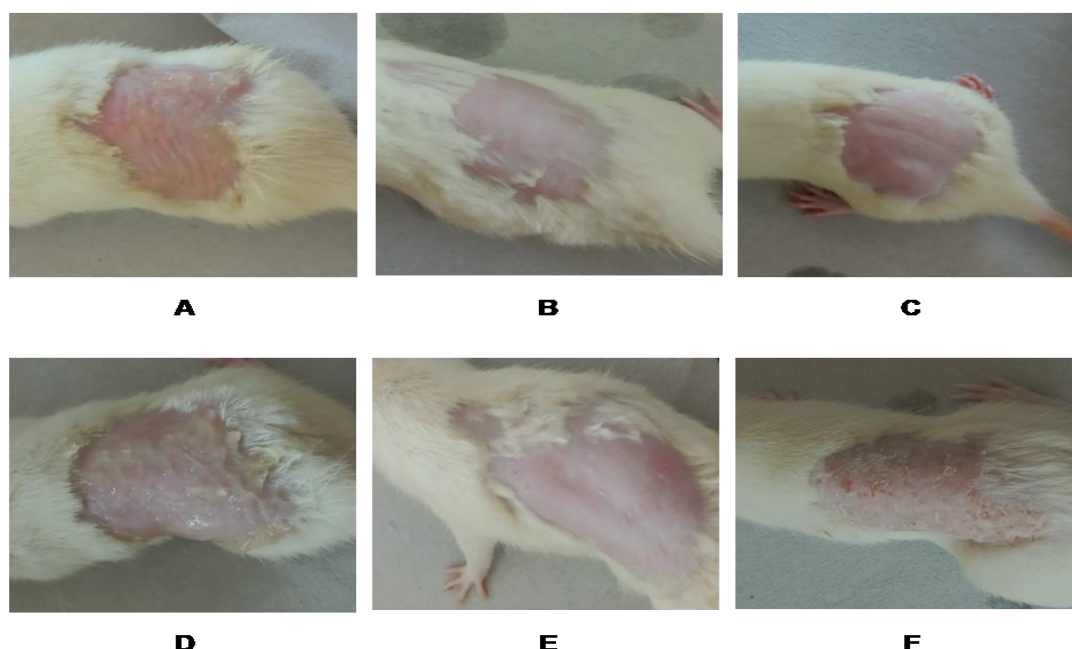


Fig. 11: Skin irritation test results: A, B and C showing skin after application of gel, after 24hrs and after 48 hrs respectively for control group; D, E and F for test group.

Table 10:Data on stability studies of film forming gel.

Form. code	Time period	Parameters evaluated	Storage temperature and relative humidity (25 \pm 3°C, 60% RH)
TG	At the end of 4 weeks	Visual appearance	Pale white, Smooth gel
		Drug content (mg/cm ²)	95 \pm 0.13
		Drug release (%)	34.406

TG: Transethosomal gel.

Conclusion

TE of DOM were formulated successfully by varying concentrations of soya lecithin and ethanol, which was then incorporated into a TG. The optimized formulation had low vesicular size, low PDI, negative ZP and high %EE. The in vitro drug release study revealed that the prepared TG had lower and sustained release than CG formulation. The ex vivo permeation

study revealed that the TG has higher permeation and flux values compared to CG. The prepared TG was also found safe to be applied to the skin surface and the stability studies showed that TG had satisfactory stability values. Therefore, it can be concluded that TG is a promising formulation for sustained transdermal delivery of DOM for the symptomatic treatment of nausea and vomiting.

Acknowledgements

The authors thank the NGSIM Institute of Pharmaceutical Sciences, Mangalore, for providing the necessary research facilities. The authors also thank STIC, Kochi, for performing SEM & TEM analysis.

REFERENCES

1. Cancer: symptoms, stages, types and what it is, (2022).
2. How does chemo work? types of chemotherapy.
<https://www.cancer.org/treatment/treatments-and-side-effects/treatment-types/chemotherapy/how-chemotherapy-drugs-work.html> (accessed on 5 August 2022).
3. İ. Altun and A. Sonkaya, "The most common side effects experienced by patients were receiving first cycle of chemotherapy", *Iran J Public Health*, 47(8),1218 (2018).
4. R.N. Brogden, A.A. Carmine, R.C. Heel, T.M. Speight and G.S. Avery, "Domperidone. A review of its pharmacological activity, pharmacokinetics and therapeutic efficacy in the symptomatic treatment of chronic dyspepsia and as an antiemetic". *Drugs*, 24(5), 360–400 (2012).
5. S.C. Reddymasu, I. Soykan, R.W. McCallum, "Domperidone: review of pharmacology and clinical applications in gastroenterology", *Am J Gastroenterol*, 102(9), 2036-2045 (2007).
6. M. Zheng, J. Chen, G. Chen, A. Farajtabar and H. Zhao, "Solubility modelling and solvent effect for domperidone in twelve green solvents", *J Mol Liq*, 261, 50–56 (2018).
7. W. Sakran, R.S. Abdel-Rashid, F. Saleh, R. Abdel-Monem, "Ethosomal gel for rectal transmucosal delivery of domperidone: design of experiment, in vitro, and in vivo evaluation", *Drug Deliv*, 29(1),1477–1491 (2022).
8. Domperidone (oral route) proper use - Mayo Clinic, (accessed on 11 August 2022).
9. A. Z. Alkilani, M.T.C. McCrudden and R.F.Donnelly, "Transdermal drug delivery: innovative pharmaceutical developments based on disruption of the barrier properties of the stratum corneum", *Pharmaceutics*, 7(4), 438 (2015).
10. T. Han and D. B.Das, "Potential of combined ultrasound and microneedles for enhanced transdermal drug permeation: a review", *Eur J Pharm Biopharm*, 89, 312–28 (2015).
11. K. Kathe and H. Kathpalia, "Film forming systems for topical and transdermal drug delivery", *Asian J Pharm Sci*, 12(6),487–497 (2017).
12. L. Kumar, S. Verma, K. Singh, D.N. Prasad and A.K.Jain, "Ethanol based vesicular carriers in transdermal drug delivery: nanoethosomes and transethosomes in focus", *Nano World J*, 2(3), 41–51 (2016).
13. A. Ascenso, S. Raposo, C. Batista, P. Cardoso, T. Mendes, F. G. Praça, M.V. Bentley, S. Simoes, "Development, characterization, and skin delivery studies of related ultradeformable vesicles: transfersomes, ethosomes, and transethosomes", *Int J Nanomedicine*, 10,5837-5851 (2015).
14. S. Goindi, B. Dhatt and A. Kaur, "Ethosomes-based topical delivery system of antihistaminic drug for treatment of skin allergies", *J Microencapsul*, 31(7), 716-724 (2014).
15. I. M. Fukuda, C.F. Pinto, C.D. Moreira, A .M. Saviano and F. R. Lourenço, "Design of experiments (DoE) applied to pharmaceutical and analytical quality by design (QbD)", *Braz J Pharm Sci*, 54, 1006 (2018).
16. I.M. Abdulbaqi, Y. Darwis, R.A. Assi, N.A.K. Khan, "Transethosomal gels as carriers for the transdermal delivery of colchicine: statistical optimization, characterization, and ex vivo evaluation", *Drug Des Devel Ther*, 12, 795-813 (2018).
17. Z.X. Chen, B. Li, T. Liu, X. Wang, Y. Zhu, L. Wang, X.H. Wang, X. Niu, Y. Xiao and Q. Sun, "Evaluation of paeonol-loaded transethosomes as

- transdermal delivery carriers", *Eur J Pharm Sci*, 99, 240–245 (2017).
18. C.K. Song, P. Balakrishnan, C.K. Shim, S.J. Chung, S. Chong and D.D.Kim, "A novel vesicular carrier, transethosome, for enhanced skin delivery of voriconazole: characterization and in vitro/in vivo evaluation", *Colloids Surf B Biointerfaces*, 92, 299-304 (2012).
 19. B.A. Habib, S. Sayed and G. M. Elsayed, "Enhanced transdermal delivery of ondansetron using nanovesicular systems: fabrication, characterization, optimization and ex-vivo permeation study-Box-Cox transformation practical example", *Eur J Pharm Sci*, 115, 352-361 (2018).
 20. M. Ma, J. Wang, F. Guo, M. Lei, F. Tan, N. Li, "Development of nanovesicular systems for dermal imiquimod delivery: physicochemical characterization and in vitro/in vivo evaluation", *J Mater Sci Mater Med*, 26,191 (2015).
 21. M. Rady, I. Gomaa, N. Afifi and M. Abdel-Kader, "Dermal delivery of Fe-chlorophyllin via ultradeformable nanovesicles for photodynamic therapy in melanoma animal model", *Int J Pharm*, 548(1), 480-490 (2018).
 22. S. Shetty, J. Jose, L. Kumar and R.N. Charyulu, "Novel ethosomal gel of clove oil for the treatment of cutaneous candidiasis", *J Cosmet Dermatol*, 18(3), 862–869.
 23. M. P. Singh, B. P. Nagori, N.R. Shaw and M. Tiwari, B. Jhanwar, "Formulation development & evaluation of topical gel formulations using different gelling agents and its comparison with marketed gel formulation", *Int J Pharm Erudition*, 3(3), 1-10 (2013).
 24. L. Kumar and R. Verma, "In vitro evaluation of topical gel prepared using natural polymer", *International J Drug Deliv*, 2(1),58–63 (2010).
 25. U.V. Sera and M.V.Ramana, "In vitro skin absorption and drug release – a comparison of four commercial hydrophilic gel preparations for topical use", *The Indian Pharmacist*, 73, 356-360 (2006).
 26. A.K. Dash, "Tolnaftate", *Anal Profiles Drug Subst Excip*, 543–70 (1994).
 27. V. Kotian, M. Koland, S. Mutalik, "Nanocrystal- based topical gels for improving wound healing efficacy of curcumin", *Crystals*, 12(11), 1565 (2022).
 28. R. Raychaudhuri, A. Pandey, S. Das, S.H. Hannuri, A. Joseph, S.D. George, A.P. Vincent and S. Mutalik, "Nanoparticle impregnated self-supporting protein gel for enhanced reduction in oxidative stress: a molecular dynamics insight for lactoferrin-polyphenol interaction. *Int J BiolMacromol*, 189,100-113 (2021).
 29. M. Lukic, I. Pantelic and S. D. Savic, "Toward optimal pH of the skin and topical formulations: from the current state of the art to tailored products. *Cosmetics*", 8(3),69 (2021).
 30. K. Babita, V. Kumar, V. Rana, S. Jain and A. K. Tiwary, "Thermotropic and spectroscopic behavior of skin: relationship with percutaneous permeation enhancement", *Curr Drug Deliv*, 3(1), 95-113 (2006).
 31. E. Abd, S.A. Yousef, M.N. Pastore, K. Telaprolu, Y.H. Mohammed, S. Namjoshi, J.E. Grice and M.S. Roberts, "Skin models for the testing of transdermal drugs", *Clin Pharmacol*, 8,163-176 (2016).
 32. S. Ghanbarzadeh and S.Arami, "Enhanced transdermal delivery of diclofenac sodium via conventional liposomes, ethosomes, and transfersomes", *Bio Med Res Int*, 2013, 1–7 (2013).
 33. J. Shaji and R.Bajaj, "Optimization and characterization of 5-fluorouracil transethosomes for skin cancer therapy using response surface methodology", *Int J Adv Res*, 6(3),1225-1233 (2018).
 34. R. Parhi and V.V.N.Goli, "Design and optimization of film-forming gel of etoricoxib using research surface methodology", *Drug Deliv Transl Res*, 10(2), 498-514 (2020).
 35. N.N. Vij and R.B.Saudagar, "Formulation, development and evaluation of film-forming gel for

- prolonged dermal delivery of terbinafine hydrochloride", *Int J Pharm Sci Res*, 5(09), 537–554 (2014).
36. A. Zafar, N.K. Alruwaili, S.S. Imam, M. Yasir, O.A. Alsaidan, A. Alquraini, A. Rawaf, B. Alsuwayt, M.K. Anwer, S. Alshehri and M. M. Ghoneim, "Development and optimization of nanolipid-based formulation of diclofenac sodium: in vitro characterization and preclinical evaluation", *Pharmaceutics*, 14(3), 507(2022).
 37. D. Nayak, R.M. Tawale, J.M. Aranjan, V. K. Tippavajhala, "Formulation, optimization and evaluation of novel ultra-deformable vesicular drug delivery system for an anti-fungal drug", *AAPS Pharm Sci Tech*, 21(5),140 (2020).
 38. M. Danaei, M. Dehghankhold, S. Ataei, H. Davarani, R. Javanmard, A. Dokhani, S. Khorasani and M.R. Mozafari, "Impact of particle size and polydispersity index on the clinical applications of lipidic nanocarrier systems", *Pharmaceutics*, 10(2), 57 (2018).
 39. R. Guo, X. Du, R. Zhang, L. Deng, A. Dong and Z. Jianhua, "Bioadhesive film formed from a novel organic-inorganic hybrid gel for transdermal drug delivery system", *Eur J Pharm Biopharm*, 79(3), 574-583 (2011).
 40. R. Albash, A. A. Abdelbary, H. Refai and M.A. El-Nabarawi, "Use of transethosomes for enhancing the transdermal delivery of olmesartanmedoxomil: in vitro, ex vivo, and in vivo evaluation", *Int J Nanomedicine*, 14(3), 1953 (2019).
 41. D.W. Oh, J.H. Kang, H. J. Laa, S. D. Han, M.H. Kang, Y. H. Kwon, J. H. Jun, D. W. Kim, Y. S. Rhee, J. Y. Kim, E.S. Park and C.W.Park, "Formulation and in vitro/in vivo evaluation of chitosan-based film forming gel containing ketoprofen", *Drug Deliv*, 24,1056-1066 (2017).
 42. I. M. Abdulbaqi, Y. Darwis, N.A.K. Khan, R. A. Assi and A. A. Khan, "Ethosomal nanocarriers: the impact of constituents and formulation techniques on ethosomal properties, in vivo studies and clinical trials", *Int J Nanomedicine*, 11, 2279-2304(2016).
 43. R. Wada, S.H. Hyon and Y. Ikada, "Kinetics of diffusion-mediated drug release enhanced by matrix degradation", *J Control Release*, 37(1-2), 151-160 (1995).
 44. S. Dash, P.N. Murthy, L. Nath and P. Chowdhury, "Kinetic modelling on drug release from controlled drug delivery systems", *Acta Pol Pharm Drug Res*, 67(3), 217-223 (2010).
 45. J. H. Lee and Y.Yeo, "Controlled drug release from pharmaceutical nanocarriers", *Chem Eng Sci*, 125, 75-84 (2015).
 46. K.V. Thorat, P. Khade, S. Kakade and A. Bhosale, "Formulation and evaluation of fast dissolving mouth film of domperidone", *World J Pharm Res*, 10(12), 2104-2121 (2021).



نشرة العلوم الصيدلانية جامعة أسيوط



تصميم وتوصيف هلام مكون للفيلم يحتوي على جسيمات ترانسفيروسومات محملة بالدومبيريدون للتوصيل عبر الجلد

سامانثا نيهيا سيكويرا - سنيه برياً*

جامعة Nitte ، معهد NGSM للعلوم الصيدلانية (NGSMIPS)، قسم المستحضرات الصيدلانية ، مانجالور ،
الهند

يهدف هذا البحث إلى صياغة هلام مكون للفيلم يحتوي على جسيمات ترانسفيروسومات محملة بالدومبيريدون - وهو دواء مضاد للقيء ومضاد للغثيان. تم تقييم الجسيمات المدخلة وكان حجم الحويصلة و PDI و % EE الأمثل 15,1 نانومتر و 0,387 و 73,82 على التوالي حيث كان الخطأ % ± 5 من القيمة المتوقعة. تم تقييم التركيبة المحضرة أيضاً من حيث جهد زيتا والفحص المجهرى الضوئى والمجهر الإلكتروني النافذ. ثم تم دمج الأنظمة الحويصلية النانوية في هلام مكون للفيلم وتقييمها لإطلاق الدواء في المختبر ودراسات نفاذية الجلد خارج الجسم الحي.